Lattice location study of ion implanted Sn and Sn-related defects in Ge

S. Decoster,[1,*] S. Cottenier,[2] U. Wahl,[3] J. G. Correia,[3] and A. Vantomme[1]

[1]*Instituut voor Kern- en Stralingsfysica and INPAC, K.U.Leuven, 3001 Leuven, Belgium*

[2]*Center for Molecular Modeling, Ghent University, Technologiepark 903, 9052 Zwijnaarde, Belgium*

[3]*Instituto Tecnológico e Nuclear, Unidade de Física e Aceleradores, Estrada Nacional 10, Apt. 21, 2686-953 Sacavém, Portugal*

(Received 13 January 2010; revised manuscript received 23 March 2010; published 14 April 2010)

In this work, we present a lattice location study of Sn in Ge. From emission channeling experiments, we determined the exact lattice location of ion implanted ^{121}Sn atoms and compared the results to predictions from density-functional calculations. The majority of the Sn atoms are positioned on the substitutional site, as can be expected for an isovalent impurity, while a second significant fraction occupies the sixfold coordinated bond-centered site, which is stable up to at least 400 °C. Corroborated by *ab initio* calculations, we attribute this fraction of bond-centered Sn atoms to the Sn-vacancy defect complex in the split-vacancy configuration. Furthermore, we are able to assign specific defect complex geometries to resonances from earlier Mössbauer spectroscopy studies of Sn in Ge.

DOI: 10.1103/PhysRevB.81.155204 PACS number(s): 61.72.uf, 61.72.jd, 61.72.Bb

I. INTRODUCTION

Ge is considered as an important future material to replace Si in semiconducting applications. Compared to Si, Ge has a higher free-carrier mobility and a lower dopant activation temperature,[1] which makes it an attractive material in future metal-oxide semiconductor field-effect transistors.[2,3] To control the growth of Ge-based devices, a thorough understanding of the diffusion properties and mechanisms is needed. It is generally accepted that most group III and V dopants (with the exception of B) in Ge diffuse by vacancy mediation. Among all impurities in group IV semiconductors, the diffusion behavior of Sn is one of the most interesting to investigate: Sn is an isovalent impurity in Ge, which means that its diffusion properties are likely to be related to Ge self-diffusion. Moreover, the investigation of Sn-related defects in Ge is a technologically important issue since Sn_xGe_{1-x} is known as a direct band gap semiconductor composed entirely of group IV elements.[4] The tunability of its band gap makes Sn_xGe_{1-x} a highly interesting material for infrared applications, especially at low Sn concentrations ($x<0.20$).[5] Recent theoretical calculations indicate that strained Sn_xGe_{1-x} ($x<0.10$) exhibits enhanced electron and hole mobility, which could make this alloy also interesting for high-speed integrated circuits.[6]

A number of studies have been performed to investigate the diffusion of Sn in Ge with secondary ion mass spectrometry.[7,8] More recently, using a radiotracer technique, Riihimäki *et al.* explained the diffusion mechanism of Sn in Ge by assuming an attractive elastic interaction between the Sn atoms and vacancies. They demonstrated that Sn diffusion is mediated by vacancies, and that the Sn-vacancy complex is negatively charged in Ge.[9,10] Although it is clear that Sn diffusion is mediated by vacancies, little is known about the microscopic configuration of Sn atoms in Ge, in particular when they are part of small defect complexes, such as the Sn-vacancy complex. It is generally accepted that the majority (if not all) of the Sn atoms are located substitutionally in a Ge matrix due to its isovalency. So far, most of the experimental information about the lattice site location of Sn and Sn-related defects in Ge is obtained from Mössbauer spectroscopy (MS) and Rutherford backscattering spectrometry in channeling geometry (RBS/C). Taraci *et al.* used RBS/C experiments to investigate the lattice location of Sn in Sn_xGe_{1-x} layers with different concentrations ($x=0.02$, 0.06, and 0.12), resulting in the observation of Sn atoms on the substitutional site only.[11] By combining MS and RBS/C experiments, Weyer *et al.* found that 90% of the ^{119m}Sn atoms were located substitutionally after implantation at 450 °C.[12] However, after implantation of ^{119}Cd, ^{119}In, ^{119}Sb, and ^{119m}Te as precursors for Sn, the Mössbauer spectra for Sn were found to consist of several contributions (resonances) with the most pronounced line interpreted as substitutional Sn and the others as several other configurations, such as isolated tetrahedral interstitial Sn atoms and two different Sn-vacancy complexes.[13–15] Although in MS experiments the Sn atoms may inherit the geometrical structure of the defects of the parent isotopes, it is still possible to measure the hyperfine parameters of the Sn atoms on different lattice sites and in several defect complexes. However, it should be pointed out that, from MS alone, it is not possible to unambiguously determine the microscopic configuration of such defect complexes.

The situation is different in theoretical work, where the atomic arrangement in a specific complex, e.g., the Sn-vacancy complex, can be imposed. The two simplest configurations for such an impurity-vacancy complex have been studied with density-functional theory:[16] (a) the so-called *full-vacancy* configuration in which the impurity is located on a substitutional site with a vacancy as nearest neighbor, and (b) the *split-vacancy* configuration where the impurity atom occupies the bond-centered (BC) site in between two vacant nearest-neighbor sites. These configurations are schematically represented in Figs. 1(a) and 1(b), respectively.

Höhler *et al.* found that in Ge the split-vacancy configuration is energetically the most favorable one for the high-Z elements Cd, In, Sn, Sb, and Bi, while the full-vacancy configuration is preferred for the lower-Z elements Al, Si, P, Ga, As, and Se.[16] One year later, comparable calculations were performed by Coutinho *et al.*, where all studied donor-

 ©2010 The American Physical Society

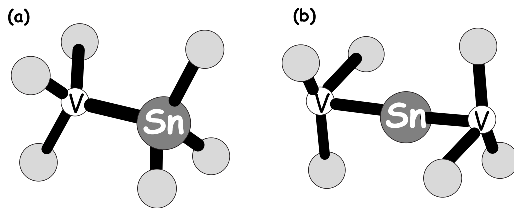

FIG. 1. Schematic presentation of the Sn-vacancy complex in Ge (a) in the full-vacancy configuration, i.e., with the Sn atom on the substitutional site, and (b) in the split-vacancy configuration, i.e., with the Sn atom on the bond-centered site.

vacancy complexes (P, As, Sb, and Bi) were calculated to be in the full-vacancy configuration in Ge.[17] According to Coutinho *et al.*, the contradicting results for the high-Z elements Sb and Bi are attributed to the size of the supercell and the k-point sampling method.

Hence, it is clear from the literature that experimental information about the microscopic structure of Sn-vacancy complexes in Ge is largely lacking, while the theoretical results on this topic, obtained by Höhler *et al.*, have been put into question. Although electron paramagnetic resonance experiments in Si have indicated that the Sn atom occupies the bond-centered site in a Sn-vacancy complex,[18] no unambiguous experimental evidence concerning the microscopic configuration of the Sn-vacancy complex in Ge has been provided so far.

In this work, we have studied the exact lattice location of ion implanted Sn atoms, both experimentally—using the emission channeling (EC) technique—and theoretically. The use of ion implantation assures that a large number of vacancies, which are known to be mobile at room temperature,[19] are present, enhancing the probability to create Sn-vacancy complexes. Recent emission channeling experiments with the optical dopant Er, the electrical dopant In and the transition metals Fe, Cu, and Ag in germanium, have proven that this technique is a very powerful tool to determine the lattice location of impurities and impurity-related defects in a direct way.[20–22] Besides emission channeling experiments, we have also performed theoretical calculations to determine the heat of formation and the hyperfine parameters of the relaxed configurations with Sn atoms on several high-symmetry sites and in several simple defect complexes in Ge. These calculations are performed using a different k-point sampling method and a larger supercell with respect to Ref. 16, as proposed by Coutinho *et al.*,[17] in order to validate our experimental results. Furthermore, these calculations will allow us to compare the deduced hyperfine parameters (isomer shift and quadrupole splitting) of the Sn atoms to the experimental values obtained from Mössbauer spectroscopy experiments.[13–15]

II. EXPERIMENTAL METHOD

EC makes use of the fact that charged particles (in this case electrons), emitted from implanted radioactive isotopes, are guided by the potential of atomic rows and planes while traveling through a single crystal. The resulting anisotropic electron emission patterns around low-index crystal directions are characteristic for the lattice site occupied by the emitting atom and are measured with a two-dimensional energy- and position-sensitive Si detector of 22×22 pixels. Applying this technique, it becomes possible to measure the lattice location of impurities with a very high accuracy (<0.02 nm) and with a sensitivity up to four orders of magnitude higher than for ion channeling spectroscopy (RBS/C). More information about the technique can be found in the paper by Wahl *et al.*[23] To obtain unambiguous quantitative results of the lattice location of the impurity under investigation, the electron emission patterns are measured around four independent crystal directions ($\langle 100\rangle$, $\langle 111\rangle$, $\langle 211\rangle$, and $\langle 110\rangle$), analyzed consistently and fitted to a set of simulated patterns. These simulations[24] are based on the dynamical theory of electron diffraction and are calculated for the substitutional (S), tetrahedral interstitial (T), BC, antibonding (AB), and the so-called SP, H, Y, and C sites,[25] together with discrete displacements between all of these high-symmetry sites along the $\langle 111\rangle$ and $\langle 100\rangle$ directions.

To study the lattice location of Sn atoms in a Ge matrix, we implanted the radioactive isotope ^{121}Sn which decays to ^{121}Sb with a half life of 27 h, emitting β electrons with an end-point energy of 390 keV. The implantations were performed at the ISOLDE facility in CERN at room temperature, in undoped $\langle 111\rangle$ Ge, with an energy of 60 keV and at an offset angle of 7° with respect to the surface normal to minimize channeling during implantation. Three slightly different implantation fluences have been used: 2×10^{12}, 3×10^{12}, and 4×10^{12} Sn atoms/cm^2. The current density used during implantation was 0.3–0.4 nA/cm^2. The measurements have been performed at room temperature, and to monitor the thermal stability of the lattice location of the implanted species, spectra were taken directly after implantation as well as after 10 min annealing stages in vacuum ($<10^{-5}$ hPa) at temperatures ranging up to 400 °C.

III. EXPERIMENTAL RESULTS

Figures 2(a)–2(d) show the measured normalized electron emission patterns from the implanted ^{121}Sn atoms in Ge (3×10^{12} atoms/cm^2) around the $\langle 111\rangle$, $\langle 100\rangle$, $\langle 110\rangle$, and $\langle 211\rangle$ axes, respectively, following 300 °C annealing. All patterns are dominated by pronounced channeling effects, indicating that the majority of the probe atoms are located along the rows of atoms in the measured directions, i.e., on the S site. To investigate small contributions of other high-symmetry sites and to obtain accurate quantitative information about the fractional occupation of the lattice sites, the experimental patterns have been fitted by simulated patterns. Up to three different high-symmetry sites were used in the fitting procedure, including small displacements of these sites as well. The only high-symmetry site that, when added to the substitutional fraction, results in a significantly improved fit which is consistent in all four measured directions (a reduced χ^2 improvement of more than 4%) is the BC site. Adding a third high-symmetry site did not further improve the fit (χ^2 improvement $\leqslant 1\%$). Using slightly displaced S and/or BC sites only results in very small fit improvements,

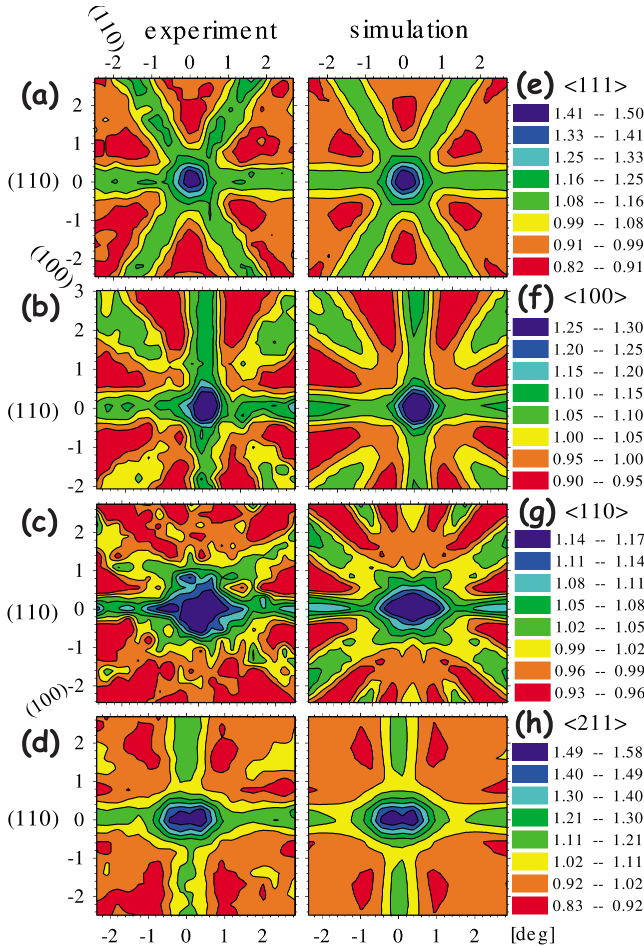

FIG. 2. (Color online) (a)–(d) Two-dimensional normalized electron emission patterns from ion implanted ^{121}Sn in Ge to a fluence of 3×10^{12} atoms/cm^2, measured around the ⟨111⟩, ⟨100⟩, ⟨110⟩, and ⟨211⟩ axes, respectively, following 300 °C annealing in vacuum; (e)–(h) the best fits to these patterns, with the majority [76(6) %] of ^{121}Sn atoms occupying the substitutional site and a smaller fraction [11(3) %] on the bond-centered site.

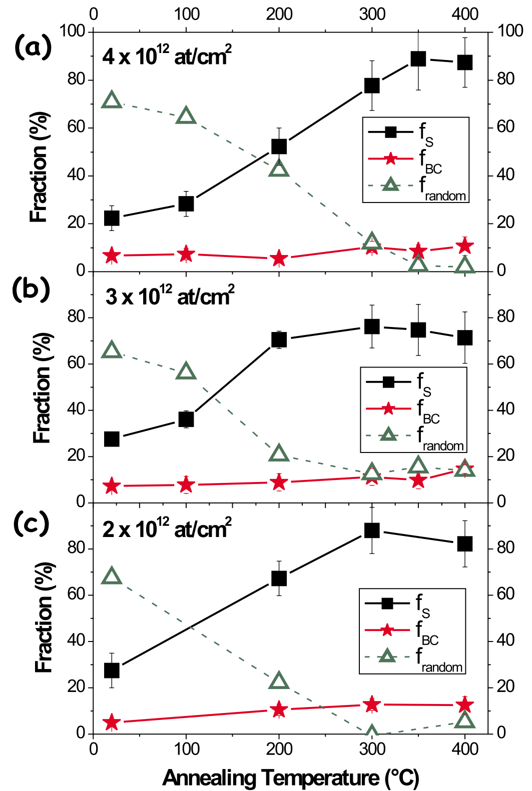

FIG. 3. (Color online) Fraction of the implanted Sn atoms on the substitutional (squares) and bond-centered (stars) sites in Ge, together with the random fraction $f_{\rm random}=100\%-f_{\rm S}-f_{\rm BC}$ (triangles) for three slightly different implantation fluences: (a) 4×10^{12}, (b) 3×10^{12}, and (c) 2×10^{12} atoms/cm^2.

which is most likely due to the extra degrees of freedom in the fitting procedure. In Figs. 2(e)–2(h), the best fits to the experimental patterns are shown, using undisplaced S and BC sites. The fractions used to produce these fits are 78%, 79%, 70%, and 75% on the S site and 11%, 9%, 14%, and 11% on the BC site for the ⟨111⟩, ⟨100⟩, ⟨110⟩, and ⟨211⟩ directions, respectively, which indicates the good consistency in the fits for the four measured directions.

As can be seen in Fig. 3, similar results are obtained for the three investigated samples, directly after implantation as well as after several annealing stages. The majority of the Sn atoms are located substitutionally ($f_{\rm S}$), with a smaller but significant fraction occupying the BC site ($f_{\rm BC}$). It is important to note the thermal stability of the Sn atoms on the bond-centered site as well as on the substitutional site, up to at least 400 °C. The remaining fraction of the Sn atoms ($f_{\rm random}=100\%-f_{\rm S}-f_{\rm BC}$) is the so-called *random fraction* and has been added to Fig. 3. This random fraction represents the Sn atoms that are not located on high-symmetry sites, only contributing to the homogeneous background of the pattern.

The results in Fig. 3 show no direct influence of the implantation fluence on the lattice location behavior of the Sn atoms, within the range of 2×10^{12}–4×10^{12} atoms/cm^2. It is clear that directly after ion implantation, a relatively high random fraction is present. This is a direct consequence of the implantation-induced lattice damage, which has a dual influence on the results shown here. First, due to the deterioration of the crystal structure, a fraction of the implanted radioactive isotopes will be located in damaged regions with reduced local crystallinity. Second, a fraction of the electrons emitted from an undamaged region will pass through damaged crystal regions, enhancing the probability for dechanneling—thus masking the impurity's lattice site. Both effects will result in an isotropic background to the patterns and consequently in the random fraction, as observed in the experiments. Therefore, the presented fractional occupation of the Sn atoms on the high-symmetry sites for the lower temperature annealing steps (<300 °C) must be regarded as a lower limit to the real values. The recovery of the lattice damage after annealing is reflected in the large decrease in the random fraction after annealing the samples at 300 °C, resulting in almost all Sn atoms on high-symmetry sites.

IV. CALCULATIONS

As expected, the majority of the isovalent Sn atoms are located substitutionally in the Ge lattice. Most likely, many

TABLE I. Calculated heats of formation ΔH_f (eV), isomer shift $\delta_{(calc)}$ (mm/s), and quadrupole splitting $\Delta E_{Q(calc)}$ (mm/s) for the relaxed impurity environments considered in this work: Sn on the S site (Sn_S), on the T site (Sn_T), on the BC site in the split-vacancy configuration [Sn_{BC} (split vacancy)], Sn on the BC site without vacancies nearby [Sn_{BC} (no vacancies)], and substitutional Sn with a self-interstitial as nearest neighbor [Sn_S+Ge_T (self-int.)]. A comparison is made to the experimental isomer shift $\delta_{(exp)}$ (mm/s) and quadrupole splitting $\Delta E_{Q(exp)}$ (mm/s) as deduced from the four Mössbauer spectroscopy lines in Refs. 13–15.

	ΔH_f (eV)	$\delta_{(calc)}$ (mm/s)	$\Delta E_{Q(calc)}$ (mm/s)	Mössbauer spectroscopy line[a,b]	$\delta_{(exp)}$ (mm/s)	$\Delta E_{Q(exp)}$ (mm/s)
Sn_S	0.19	1.75	0.0	2	1.90	0.0
Sn_T	3.96	3.19	0.0	4	3.27	0.0
Sn_{BC} (split vacancy)	1.86	2.24	0.10	3	2.36	0.3[a]–0.4[b]
Sn_{BC} (no vacancies)	3.83	3.25	0.82			
Sn_S+Ge_T (self-int.)	3.51	1.84	0.64			
unknown				1	1.41	0.0

[a]Reference 13.
[b]References 14 and 15.

of these impurities are embedded in an undamaged environment, although it cannot be excluded that some of them are surrounded by simple defects, without influencing their substitutional position. A smaller but significant fraction of Sn atoms is found to occupy the BC site, which has not been reported by experiments on Sn atoms in Ge so far. As mentioned above, this BC fraction is possibly related to the Sn-vacancy defect in the split-vacancy configuration, as presented in Fig. 1(b). To strengthen this assumption, complementary *ab initio* calculations have been performed.

We have calculated the heat of formation of several impurity sites for Sn in Ge: the S site (with and without a vacancy or a Ge self-interstitial as a nearest neighbor), the T site (with as well as without a vacancy as a nearest neighbor), and the BC site (in the split-vacancy configuration and without any vacancies nearby). All defect complexes were allowed to completely relax to their most stable configuration. The heats of formation reported in Table I are calculated according to

$$\Delta H_f = E^{imp}_{sup} - \mu_{imp} - (32E^{id}_{sup} - n\mu_{\mathrm{Ge}}), \qquad (1)$$

where E^{imp}_{sup} is the total energy of a 63- or 64-atom supercell that contains the impurity, E^{id}_{sup} is the total energy of a pure Ge unit cell (diamond structure, two atoms), μ_{Ge} is the chemical potential of Ge (taken equal to the total energy per atom in bulk Ge), n is the number of Ge atoms in the ideal 64-atom supercell that are replaced with either vacancies or impurities ($n=1,2$), and μ_{imp} is the chemical potential of Sn (taken equal to the total energy per atom in bulk α-Sn). The Ge lattice constant was optimized and fixed for the 64-atom cells. The calculations were done by the APW+lo method[26] within density-functional theory,[27] as implemented in the WIEN2K code.[28,29] The Perdew-Burke-Ernzerhof[30] exchange-correlation functional was used, the k-space sampling was done on a $4\times4\times4$ mesh in the 64-atom cell, and a basis set corresponding to $K_{max}=3.5$ a.u. was taken. The influence of the size of the supercell (up to 256 atoms) on the calculations was verified and found to be negligible. In this way, we have performed calculations in a similar way as Höhler *et al.*,[16] while also taking into account the suggestions of Coutinho *et al.*,[17] i.e., increasing the number of k points and the size of the supercell.

After relaxation of the configuration with the Sn impurity on the S site (Sn_S) and the T site (Sn_T), we found local expansions of the nearest-neighbor distance of 5% and 8%, respectively. When adding a vacancy as a nearest neighbor to the substitutional impurity, the calculations indicate a large force on the Sn atom along the ⟨111⟩ direction of the Ge crystal, resulting in the spontaneous relocation of the Sn impurity to the sixfold coordinated BC site with the vacancy *split* over the nearest-neighbor positions: the split-vacancy configuration [see Fig. 1(b)]. Although having a different k-point sampling method and an increased supercell size, these results are in agreement with what was found by Höhler *et al.*:[16] the Sn_S-vacancy complex in the full-vacancy configuration is not stable in Ge and spontaneously relaxes to the split-vacancy configuration.

When adding a nearest-neighbor vacancy to the Sn_T configuration, the interstitial Sn atom feels a force toward the vacant site. As a result, this configuration is not stable either, resulting in the relocation of the Sn atom to the substitutional site. When relaxing the configuration with Sn on the BC site and no vacancies nearby, no lattice site changes (but relatively large displacements of the surrounding Ge atoms) were observed. Finally, the configuration with a Ge self-interstitial as a nearest neighbor of a substitutional Sn impurity was found to be stable, i.e., no lattice site changes were observed.

V. DISCUSSION

By comparing the heats of formation in Table I, it is clear that the Sn atoms prefer the S site to the other high-symmetry sites. This is consistent with previous experiments where the majority of Sn atoms were found on the S site,[11,12] with our emission channeling results, and with what one would expect for isovalent impurities. Although the heats of formation in Table I suggest that Sn on the BC site is energetically not very favorable (with respect to substitutional

Sn), the following arguments show that this is not the case. We calculated the heat of formation for a single neutral vacancy in Ge to be 2.23 eV (in agreement with the literature[31]). Hence, the total energy needed to have an impurity on the S site and an isolated vacancy *not* bound to it (0.19 eV+2.23 eV=2.42 eV) is significantly larger than the heat of formation of the split-vacancy configuration of the Sn-vacancy complex (1.86 eV). This result is in agreement with the attractive interaction between Sn atoms and vacancies found by Riihimäki *et al.*[9] Therefore, one can conclude that a substitutional Sn atom will likely trap one of the abundantly available mobile vacancies created during implantation, and—as the structural relaxation process in our calculations shows—will spontaneously evolve into the BC site. Consequently, our experimental results are well corroborated by the presented *ab initio* calculations.

Additionally, in order to allow a comparison of our results with the results from the above-mentioned Mössbauer spectroscopy experiments,[13–15] we have calculated the isomer shift (relative to $CaSnO_3$) and the quadrupole splitting for ^{119}Sn atoms on several high-symmetry lattice sites, with and without a vacancy or a self-interstitial nearby. Isomer shift calculations were performed according to the common method, as described, e.g., in Refs. 32 and 33. The quadrupole splitting was determined following the standard procedure for calculating the electric field gradient as presented in Ref. 34. For each configuration, we investigated the influence of the magnetic moment (0, μ_B, and $2\mu_B$) and the charge state (2+, 1+, and 0+) of the impurity atom on the calculated hyperfine parameters. Charged states were obtained by subtracting (adding) electrons from (to) the unit cell, together with a neutralizing homogeneous background charge. The calculated values (open symbols) and experimental values from previous MS experiments (closed symbols) are presented in Fig. 4 and are also listed in Table I. For reasons of clarity, each configuration has been plotted in Fig. 4 with the same (open) symbol for different charge states and magnetic moments. As can be seen from Fig. 4, the charge state and the magnetic moment of the impurity atom do not have a significant influence on the calculated hyperfine parameters, and therefore will not be discussed in more detail.

In Refs. 13–15, four different Mössbauer resonances (labeled as lines 1–4) were identified. Lines 2 and 4 were assigned to Sn atoms in tetrahedrally symmetrical surroundings, i.e., on the S and the T sites, respectively. These assignments are in good agreement with our calculated hyperfine parameters for these sites, as can be seen from Table I and Fig. 4. Lines 3 and 1 were interpreted as Sn-vacancy complexes in the full-vacancy and split-vacancy configurations, respectively. Our calculations show that the hyperfine parameters of the bond-centered Sn atoms in the split-vacancy configuration are not in agreement with line 1, but in relatively good agreement[35] with line 3, indicating that the tentative assignment of these two Mössbauer lines was most likely incorrect. These results show that the Sn-vacancy complex in the split-vacancy configuration has been measured indirectly before, however, without having been identified as such. Since the hyperfine parameters of the other calculated configurations are not in agreement with the experimental values of line 1, it has not been possible to assign

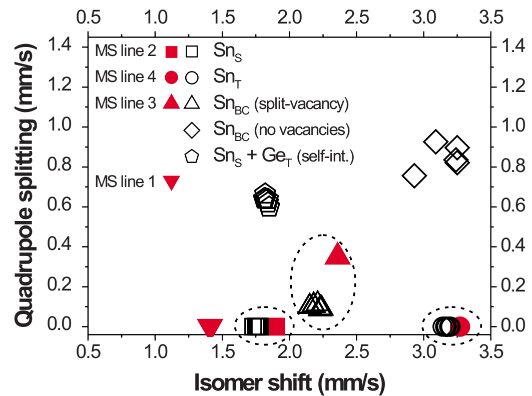

FIG. 4. (Color online) Calculated (open symbols) and measured (Refs. 13–15) (closed symbols) hyperfine parameters (quadrupole splitting versus isomer shift) of Sn impurities on the substitutional site (Sn_S, squares), on the tetrahedral interstitial site (Sn_T, circles), on the bond-centered site in the split-vacancy configuration [Sn_{BC} (split vacancy), up triangles], on the bond-centered site without vacancies nearby [Sn_{BC} (no vacancies), diamonds], and on the substitutional site with a self-interstitial as nearest neighbor [Sn_S+Ge_T (self-int.), pentagons]. For each configuration, the calculations have been performed for different charge states and magnetic moments, but for reasons of clarity, the charge state and magnetic moment of each calculation are not explicitly shown in the figure and represented by multiple (open) symbols.

a specific configuration to this Mössbauer resonance. As a general quality check, we note that the isomer shift values calculated by Höhler *et al.*—i.e., 1.88 mm/s for substitutional Sn and 2.16–2.19 mm/s for Sn in the split-vacancy configuration[16]—are in good agreement with our calculations.

VI. CONCLUSIONS

In conclusion, we have performed an experimental and theoretical lattice location study of ion implanted Sn in Ge. The majority of the isovalent Sn impurities are located substitutionally, although a significant fraction of the Sn atoms was found on the BC site. Backed up by *ab initio* density-functional calculations, we have been able to relate the bond-centered Sn atoms with Sn-vacancy complexes in the split-vacancy configuration. Moreover, calculations of the hyperfine parameters of this defect indicate that it has been present in Mössbauer experiments before, without having been identified as such. In our work, we have presented strong evidence, both experimentally and theoretically, that the Sn-vacancy defect prefers the split-vacancy configuration which is thermally stable up to at least 400 °C. This result is of major importance in the understanding of the problems that arise in the formation of diluted Sn_xGe_{1-x} alloys since recent calculations have indicated that the split-vacancy configuration of the Sn atom in Ge is a nucleation point of metallic Sn,[36] hence deteriorating the semiconducting properties. Besides this, our results contribute to the study of simple point defects in elemental group IV semiconductors and are important to understand the vacancy-mediated mechanism of Sn diffusion—and maybe even self-diffusion—in germanium.

The conclusions obtained here for Sn in Ge can be compared with previous results for the transition metals Fe, Cu, and Ag, and the acceptor In, which were experimentally observed and calculated to be on the BC site in the impurity-vacancy complex in Ge as well.[16,21,22] Therefore, a general trend can be expected for the transition metals, group III and IV impurities in Ge. However, preliminary results of similar calculations for group V impurity-vacancy complexes indicate that this trend cannot be generalized for all impurities in Ge, highlighting the need of additional experimental and theoretical studies on impurity-vacancy complexes in Ge.

ACKNOWLEDGMENTS

This work was supported by the Research Foundation–Flanders (FWO G.0501.07 and G.0636.08), the Concerted Action of the K.U.Leuven (GOA/2009/006), the Inter-University Attraction Pole (IUAP P6/42), the Center of Excellence Programme (INPAC EF/2005/005), the Portuguese Foundation for Science and Technology (CERN-FP-109272-2009), and the ISOLDE collaboration. S.D. acknowledges FWO and the Research Council of the K.U.Leuven.

---

*stefan.decoster@fys.kuleuven.be

[1] R. Hull and J. C. Bean, *Germanium Silicon: Physics and Materials, Semiconductors and Semimetals* (Academic, San Diego, 1999).

[2] C. C. Yeo, B. J. Cho, F. Gao, S. J. Lee, M. H. Lee, C. Y. Yu, C. W. Liu, L. J. Tang, and T. W. Lee, IEEE Electron Device Lett. **26**, 761 (2005).

[3] Y. J. Yang, W. S. Ho, C. F. Huang, S. T. Chang, and C. W. Liu, Appl. Phys. Lett. **91**, 102103 (2007).

[4] C. H. L. Goodman, IEE Proc., Part I: Solid-State Electron Devices **129**, 189 (1982).

[5] G. He and H. A. Atwater, Phys. Rev. Lett. **79**, 1937 (1997).

[6] J. D. Sau and M. L. Cohen, Phys. Rev. B **75**, 045208 (2007).

[7] P. Kringhøj and R. G. Elliman, Appl. Phys. Lett. **65**, 324 (1994).

[8] M. Friesel, U. Sodervall, and W. Gust, J. Appl. Phys. **78**, 5351 (1995).

[9] I. Riihimäki, A. Virtanen, H. Kettunen, P. Pusa, P. Laitinen, J. Räisänen, and the ISOLDE Collaboration, Appl. Phys. Lett. **90**, 181922 (2007).

[10] I. Riihimäki, A. Virtanen, S. Rinta-Anttila, P. Pusa, J. Räisänen, and the ISOLDE Collaboration, Appl. Phys. Lett. **91**, 091922 (2007).

[11] J. Taraci, S. Zollner, M. R. McCartney, J. Menendez, M. A. Santana-Aranda, D. J. Smith, A. Haaland, A. V. Tutukin, G. Gundersen, G. Wolf, and J. Kouvetakis, J. Am. Chem. Soc. **123**, 10980 (2001).

[12] G. Weyer, A. Nylandsted-Larsen, B. I. Deutch, J. U. Andersen, and E. Antoncik, Hyperfine Interact. **1**, 93 (1975).

[13] G. Weyer, S. Damgaard, J. W. Petersen, and J. Heinemeier, Phys. Lett. **76A**, 321 (1980).

[14] G. Weyer, J. W. Petersen, and S. Damgaard, Hyperfine Interact. **10**, 775 (1981).

[15] S. Damgaard, A. F. F. Olesen, J. W. Petersen, and G. Weyer, Phys. Scr. **22**, 640 (1981).

[16] H. Höhler, N. Atodiresei, K. Schroeder, R. Zeller, and P. H. Dederichs, Phys. Rev. B **71**, 035212 (2005).

[17] J. Coutinho, S. Öberg, V. J. B. Torres, M. Barroso, R. Jones, and P. R. Briddon, Phys. Rev. B **73**, 235213 (2006).

[18] G. D. Watkins, Phys. Rev. B **12**, 4383 (1975).

[19] H. Haesslein, R. Sielemann, and C. Zistl, Phys. Rev. Lett. **80**, 2626 (1998).

[20] S. Decoster, B. De Vries, U. Wahl, J. G. Correia, and A. Vantomme, Appl. Phys. Lett. **93**, 141907 (2008).

[21] S. Decoster, S. Cottenier, B. De Vries, H. Emmerich, U. Wahl, J. G. Correia, and A. Vantomme, Phys. Rev. Lett. **102**, 065502 (2009).

[22] S. Decoster, B. De Vries, U. Wahl, J. G. Correia, and A. Vantomme, J. Appl. Phys. **105**, 083522 (2009).

[23] U. Wahl, J. G. Correia, A. Czermak, S. G. Jahn, P. Jalocha, J. G. Marques, A. Rudge, F. Schopper, J. C. Soares, A. Vantomme, P. Weilhammer, and the ISOLDE Collaboration, Nucl. Instrum. Methods Phys. Res. A **524**, 245 (2004).

[24] H. Hofsäss and G. Lindner, Phys. Rep. **201**, 121 (1991).

[25] U. Wahl, J. G. Correia, A. Vantomme, G. Langouche, and the ISOLDE Collaboration, Physica B **273-274**, 367 (1999).

[26] E. Sjöstedt, L. Nordström, and D. J. Singh, Solid State Commun. **114**, 15 (2000).

[27] P. Hohenberg and W. Kohn, Phys. Rev. **136**, B864 (1964).

[28] S. Cottenier, *Analysis of an Electric Field Gradient (EFG): the EFG switch in LAPW2* (Instituut voor Kern- en Stralingsfysica, K.U.Leuven, Leuven, 2002); freely available from http://www.wien2k.at/reg_user/textbooks

[29] P. Blaha, K. Schwarz, G. Madsen, D. Kvasnicka, and J. Luitz, *Wien2k: An Augmented Plane Wave plus Local Orbitals program for calculating crystal properties* (Karlheinz Schwarz, TU Wien, Wien, 2001).

[30] J. P. Perdew, K. Burke, and M. Ernzerhof, Phys. Rev. Lett. **77**, 3865 (1996).

[31] J. Vanhellemont, P. Spiewak, and K. Sueoka, J. Appl. Phys. **101**, 036103 (2007).

[32] A. Svane, N. E. Christensen, C. O. Rodriguez, and M. Methfessel, Phys. Rev. B **55**, 12572 (1997).

[33] P. E. Lippens, Phys. Rev. B **60**, 4576 (1999).

[34] P. Blaha, K. Schwarz, and P. H. Dederichs, Phys. Rev. B **37**, 2792 (1988).

[35] Due to the relatively small quadrupole moment (0.132 b) of ^{119}Sn, a small electric field gradient results in an unresolved doublet in MS measurements, i.e., a line which is only slightly broader than the natural linewidth. This makes an accurate experimental determination of the quadrupole splitting very difficult, which might be the reason for the relatively large difference between the calculated and the experimentally observed quadrupole splitting. However, since the experimental value of the isomer shift, which can be determined much more accurately, is very close to the calculated value, we can still conclude that the experimental and calculated hyperfine parameters of Sn_{BC} in the split-vacancy configuration are in good agreement.

[36] C. I. Ventura, J. D. Fuhr, and R. A. Barrio, Phys. Rev. B **79**, 155202 (2009).